GSICS Global Space-based Inter-Calibration System

Quarterly

Newsletter Summer 2022 Issue

doi: 10.25923/7kkg-vz09
Vol. 16 No 2, 2022
Editor: Manik Bali ESSIC/UMD

CMA • CNES • ESA • EUMETSAT • IMD • ISRO • JAXA • JMA • KMA • NASA • NIST • NOAA • ROSCOSMOS . ROSHYDROMET • SITP • USGS • WMO

Using visible and near-infrared satellite channels in NWP

By L. Scheck (DWD/HErZ), F. Baur (DWD/HErZ), C. Stumpf (DWD), C. Köpken-Watts (DWD), S. Geiss (LMU), L. Bach (DWD), A. de Lozar (DWD), M. Weissmann (University of Vienna)

Satellite images provide high-resolution information on the state of the atmosphere that is well-suited for data assimilation and model evaluation. So far only thermal infrared channels containing temperature, humidity and cloud information are directly assimilated. However, the solar channels contain interesting, complementary information. For instance, visible channels provide much better information on the water or ice contents of clouds, as they saturate only at considerably higher water paths than infrared channels. Near-infrared channels are particularly sensitive to effective cloud droplet or ice particle sizes and the 1.6µm near-infrared channel allows for distinguishing water from ice clouds.

Solar channels have not been assimilated in operational systems, mainly because suitable forward operators were missing. In the solar spectral range multiple scattering is important and cannot be treated using computationally efficient approximations that work in the infrared range. Consequently, standard radiative transfer (RT) methods are orders of magnitude too slow for operational purposes. As a further complication, 3D RT effects can be important in the solar range, and 3D RT solvers are computationally even more expensive.

Forward operator design

The development of a fast forward operator for visible channels started at LMU Munich and is now continued jointly by LMU and DWD in the framework of the Hans Ertel Centre for Weather Research (HErZ). The Method for Fast Satellite Image Synthesis (MFASIS, Scheck et al. 2016) makes use of the fact that for non-absorbing visible details of the vertical cloud structure are not important. It is therefore sufficient to describe the RT problem for each model column by only eight parameters, water and ice total optical depths and mean effective particle radii, three angles to describe the geometry and a surface albedo. This makes it feasible to precompute an eight-dimensional reflectance look-up table (LUT) using standard methods and to just interpolate in the LUT to determine reflectances. A lossy compression approach is used to bring the LUT size from 8GB down to 21MB. MFASIS was implemented in the RTTOV-13 package (Saunders et al. 2020) and has since been improved further, e.g. to reduce reflectance errors in the presence of mixed phase clouds.

For channels in which absorption plays a role, and for taking aerosols into account, additional LUT dimensions are required, but would lead to strongly increased LUT sizes. Neural networks were investigated as a more efficient alternative to LUTs by Scheck (2021), who demonstrates that relatively small networks with the same input

doi: 10.25923/7kkg-vz09

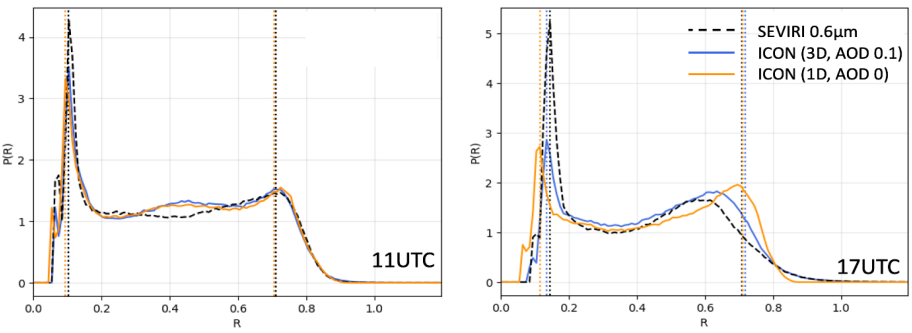

Figure 1. Probability distribution functions of observed (black dashed) and simulated 0.6µm SEVIRI reflectances at 11 UTC (left panel) and 17 UTC (right panel) for a 30-day period. Results with (blue) and without (orange) 3D RT effects and aerosols are compared.

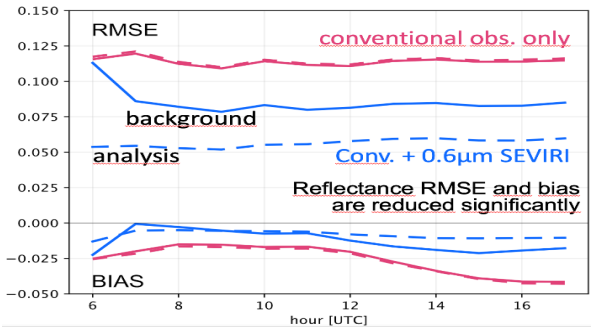

Figure 2 . Average 0.6µm reflectance RMSE (upper lines) and bias (lower lines) for the analysis (dashed) and the first guess (solid) as a function of the time of the day for 30-day ICON-D2 LETKF experiments in which only conventional observation (red) or conventional observations and visible reflectances (blue) were assimilated.

parameters as in MFASIS can be trained to generate reflectances with even higher accuracy. Moreover, the neural networks are an order of magnitude faster and require much less reflectance data to be generated with slow standard methods. Work is in progress to use the promising new approach for the 1.6µm channel and for aerosols.

In addition, a forward operator extension has been developed to approximate the most important 3D RT effect: For cloud tops tilted towards / away from the sun the reflectance is increased / reduced. Using a transformation into a rotated frame of reference aligned with the cloud top the impact of the tilt on the reflectance can be estimated efficiently (Scheck et a. 2018) and errors compared to 3D RT reference calculations can be reduced.

First model evaluation and data assimilation results

In a recent model evaluation study, Geiss et al. (2021) computed SEVIRI 0.6µm images from 30-day hindcasts for a summer period performed with the regional ICON-D2 model. The 0.6µm observations turned out to be very helpful for tuning the subgrid cloud scheme. After taking a constant aerosol background and 3D effects into account, the agreement between observed and synthetic reflectance distributions is now quite good, at least for not too extreme solar zenith angles (Fig. 1). Preliminary results for the global ICON model indicate somewhat larger errors but in general also a reasonable agreement of observed and synthetic distributions. Monitoring studies for visible channels are also in progress at ECMWF.

MFASIS has also been used in first data assimilation experiments with DWDs regional Kilometer-Scale Ensemble Data Assimilation (KENDA) system. Scheck et al. 2020 demonstrated for SEVIRI 0.6µm observations that in single observation experiments model clouds are improved and explored different assimilation settings. In recent assimilation experiments using a near-operational setup it was confirmed that the location and thickness of clouds (and therefore also surface radiation) are strongly improved (Fig. 2) in the analysis and that for several hours also in the forecast.

References:

Geiss, S., et al., 2021, Understanding the model representation of clouds based on visible and infrared satellite observations, ACP, DOI: 10.5194/acp-21-12273-2021

Scheck, L., 2021: A neural network based forward operator for visible satellite images and its adjoint, JQSRT, DOI: 10.1016/j.jqsrt.2021.107841

Saunders et al., 2020, RTTOV-13 Science and validation report, rttov13_svr.pdf

Scheck, L., Weissmann, M. and Bach, L., 2020, Assimilating visible satellite images for convective-scale numerical weather prediction: A case study, Q. J. R. Meteorol. Soc., 146: 3165– 3186, DOI: 10.1002/qj.3840.

Scheck, L., Weissmann, M., Mayer, B., 2018, Efficient methods to account for cloud top inclination and cloud overlap in synthetic visible satellite images, JTECH, Vol. 35, Issue: 3, p. 665-685, DOI: 10.1175/JTECH-D-17-0057.1

Scheck, L., Frerebeau, P., Buras-Schnell, R., Mayer B., 2016, A fast radiative transfer method for the simulation of visible satellite imagery, JQSRT, 175, p. 54-67, DOI: 10.1016/j.jqsrt.2016.02.008

doi: 10.25923/7kkg-vz09

In-Flight Relative Radiometric Calibration of a Wide Field of View Directional Polarimetric Camera Based on the Rayleigh Scattering over Ocean

By Sifeng Zhu, Zhengqiang Li, Lili Qie, Hua Xu (Aerospace Information Research Institute, Chinese Academy of Sciences, Beijing, PR China)

The directional polarimetric camera (DPC) is a Chinese satellite sensor with a wide field of view (FOV) to observe the polarization and directionality of the earth's reflectance, which aims to detect global atmospheric aerosol and cloud properties. The first DPC sensor was successfully launched on 9 May 2018 onboard the Chinese GaoFen-5 satellite, a sun-synchronous orbiting satellite, at an altitude of 705km with an inclination of 98◦, which has 1:30 p.m. local overpass time [1]. It is a difficult task to calibrate the in-flight relative radiometric variation of the sensors with such a wide FOV. In this study, a new method based on Rayleigh scattering over the ocean is developed to estimate the radiometric sensitivity variation over the whole FOV of DPC. The radiometric response drift of DPC / GaoFen-5 over the whole DPC FOV during its life cycle are evaluated.

DPC has a large field of view (FOV) (±50° both along-track and cross-track) and a high spatial resolution (about 3.3 km at nadir). As shown in Figure 1, DPC's optical system consists of a telecentric optic with wide FOV, a rotating wheel module carrying spectral filters and polarizers, and a bidimensional CCD detector array with 512 × 512 detectors. The multi-angular viewing of the same surface target in more than 9 angles is possible due to the over-riding of the successive images along the satellite track [2,3].

Rayleigh scattering may contribute up to 70% of the satellite observation at the TOA over a clear deep ocean region. As shown in Figure 2, the oceanic sites were selected for their pristine atmosphere, low phytoplankton concentrations, homogeneities, and moderated seasonal variations. Therefore, the apparent reflectance observed by satellite can be accurately simulated using a radiative transfer model (RTM) [4], which can be approximately expressed as follows,

$$\rho \cong \rho_m + \rho_a + (\rho_f + \rho_w + \rho_{gl})e^{-M\delta} \quad .....(1)$$

where ρ_m is the contribution of Rayleigh scattering of atmospheric molecules, ρ_a is the contribution of aerosol scattering. ρ_f and ρ_w are the contributions of water-leaving reflectance and the whitecap reflectance respectively. ρ_{gl} represents the reflectance of direct sunlight on the ocean surface. M is the air mass, and δ is the total optical thickness of the atmosphere.

Assuming that the in-flight polarization effect parameters of the optical system are stable and accurately accorded, then the in-flight/pre-flight variation of the satellite absolute radiometric coefficient is obtained,

$$A'_k = \frac{A_{k,\text{in-flight}}}{A_{k,\text{pre-flight}}} = \frac{I_{\text{mea},k}}{I_{\text{cal},k}} \quad .....(2)$$

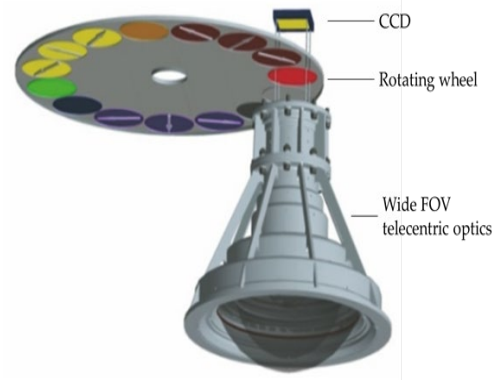

Figure 1. The optics of the DPC.

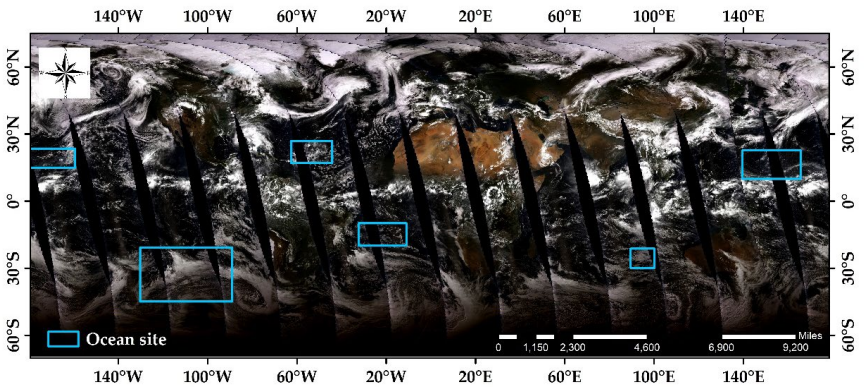

Figure 2. Location of global radiometric calibration oceanic sites for Rayleigh scattering calibration

doi: 10.25923/7kkg-vz09

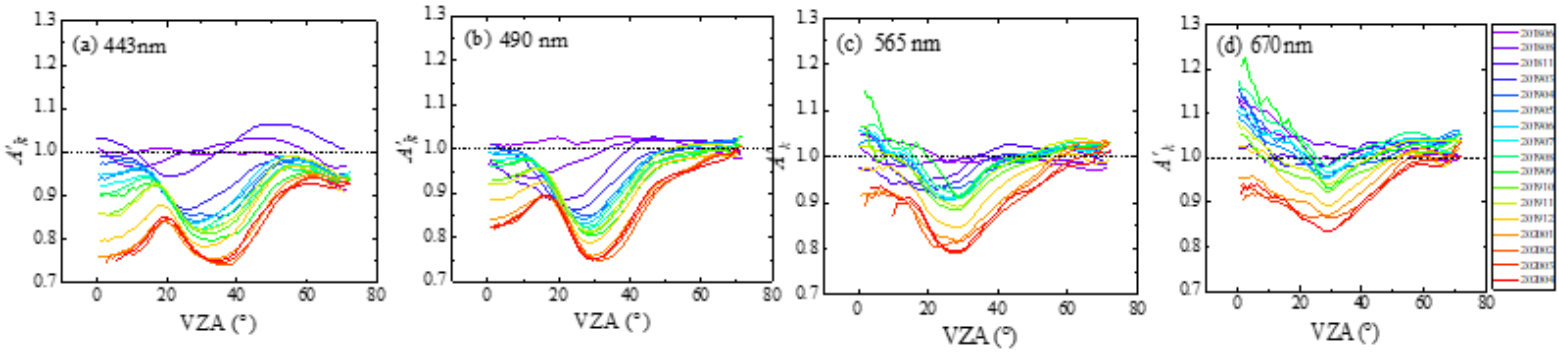

Figure. 3 The monthly average A'_k results of Rayleigh scattering calibration vary with VZA from March 2019 to April 2020 for (**a**) 443 nm, (**b**) 490 nm, (**c**) 565 nm and (**d**) 670 nm bands of DPC/GaoFen-5.

where $A_{k,\mathrm{in-flight}}$ is the in-flight absolute calibration coefficient. $A_{k,\mathrm{pre-flight}}$ is the preflight absolute calibration coefficient. $I_{\mathrm{mea},k}$ is the radiance calculated with pre-flight calibration coefficients at band k, which is obtained directly in the official Level 1 product. The $I_{\mathrm{cal},k}$ is the theoretical radiance that should be observed by the satellite sensor at the TOA, which is simulated by the RTM by inputting the sun-viewing geometry and the atmospheric and oceanic parameters. The relative radiometric calibration of DPC is defined as estimating the inconsistency sensitivity at different positions of the FOV to the same incident radiation [2]. Thanks to the large amounts of Rayleigh samples and the multi-angular observation of DPC, the relative radiometric calibration of DPC can be achieved by fitting the A'_k as a function of the viewing angles.

Firstly, the theoretical radiometric calibration uncertainty of the method, considering the typical input uncertainties for several atmospheric and oceanic parameters, is analyzed. The calibration uncertainties increase with wavelength and decrease with the viewing zenith angle, they are about 2.0 – 6.9% (depending on the wavelength) when the view zenith angle (VZA) is 0°, and decrease to about 1 – 3.8% when VZA increases to 70°. This random calibration noise caused by the input parameters error may be reduced by a large number of samples averaged.

Secondly, the method is applied to evaluate the long-term radiometric drift of the DPC. It is found that the radiometric response of DPC/GaoFen-5 over the whole FOV is progressively drifting over time. The sensitivity at shorter bands decreases more strongly than longer bands, and at the central part of the optics decreases more strongly than the marginal part. During the 14 months (from March 2019 to April 2020) of operational running in-orbit, the DPC radiometric responses of 443 nm, 490 nm, 565 nm, and 670 nm bands drifted by about 4.44 – 23.08%, 4.75 – 16.22%, 3.86 – 9.81%, and 4.7 – 16.86%, respectively, from the marginal to the central part of the FOV. The radiometric sensitivity has become more stable since January 2020. The temporal drift of the average A'_k at the central part of the FOV, with VZA less than 10°, are listed in Table 1.

Then the temporal radiometric drift of DPC/GaoFen-5 is corrected by combining the relative and absolute radiometric coefficients. The correction is convincing by cross calibration with MODIS/Aqua observation over the desert sites. After correction the mean bias of A'_k is promoted from 0.17 to 0.05 and from 0.13 to 0.05, and RMSE is promoted from 0.18 to 0.06 and from 0.15 to 0.05, for 443 nm and 490 nm bands, respectively.

At last, an application of the radiometric corrected DPC data to improve the aerosol optical depth (AOD) retrievals is performed to prove the efficiency of the correction [5]. The AOD retrievals from the corrected DPC measurements are distinctly improved when compared with ground-based Sun-

Month	A'_k(443 nm)	A'_k(490 nm)	A'_k(565 nm)	A'_k(670 nm)
2019/03	0.979	0.996	1.029	1.098
2019/04	0.963	0.99	1.029	1.071
2019/05	0.958	0.989	1.03	1.067
2019/06	0.94	0.983	1.035	1.078
2019/07	0.922	0.971	1.042	1.101
2019/08	0.911	0.966	1.062	1.14
2019/09	0.882	0.945	1.061	1.062
2019/10	0.866	0.929	1.013	1.044
2019/11	0.832	0.906	0.985	1.036
2019/12	0.81	0.892	0.976	1.02
2020/01	0.766	0.848	0.92	0.945
2020/02	0.75	0.831	0.909	0.922
2020/03	0.747	0.831	0.934	0.926

Table 1. Monthly absolute calibration coefficient A'_k from March 2019 to April 2020 at four visible bands of DPC/GaoFen-5.

photometer measurements with a linear fitting slope improved from 0.6 to 1.06 and the RMSE decreases from 0.31 to 0.21. This indicates an improvement of the radiometrically corrected data by this method.

Reference

[1] Li, Z.; Hou, W.; Hong, J.; Zheng, F.; Luo, D.; Wang, J.; Gu, X.; Qiao, Y. Directional Polarimetric Camera (DPC): Monitoring aerosol spectral optical properties over land from satellite observation. Journal of Quantitative Spectroscopy and Radiative Transfer **2018**, 218, 21-37, doi:10.1016/j.jqsrt.2018.07.003.

[2] Huang, C.; Xiang, G.; Chang, Y.; Han, L.; Zhang, M.; Li, S.; Tu, B.; Meng, B.; Hong, J. Pre-flight calibration of a multi-angle polarimetric satellite sensor directional polarimetric camera. Opt Express **2020**, 28, 13187-13215, doi:10.1364/OE.391078.

[3] Huang, C.; Chang, Y.; Xiang, G.; Han, L.; Chen, F.; Luo, D.; Li, S.; Sun, L.; Tu, B.; Meng, B.; et al. Polarization measurement accuracy analysis and improvement methods for the directional polarimetric camera. Opt Express **2020**, 28, 38638-38666, doi:10.1364/OE.405834.

[4] Vermote, E.F.; Tanré, D.; Deuze, J.L.; Herman, M.; Morcette, J.-J. Second simulation of the satellite signal in the solar spectrum, 6S: An overview. IEEE transactions on geoscience and remote sensing **1997**, 35, 675-686.

[5] Ge, B.; Li, Z.; Chen, C.; Hou, W.; Xie, Y.; Zhu, S.; Qie, L.; Zhang, Y.; Li, K.; Xu, H.; Ma, Y.; Yan, L.; Mei, X. An Improved Aerosol Optical Depth Retrieval Algorithm for Multiangle Directional Polarimetric Camera (DPC). Remote Sens. 2022, 14, 4045. https://doi.org/10.3390/rs14164045

The RAMI4ATM initiative

By Nadine Gobron[(1)], Yves Govaerts[(2)], Nicolas Misk[(2)] and Christian Lanconelli[(1,3)] [1]Joint Research Centre, [2]Rayference, [3]Uni.Systems S.A. Luxemburg

Introduction

The latest progress concerning vicarious calibration over bright desert pseudo-invariant calibration site (PICS) allows reaching an accuracy of about 3 to 5% when applied on many cloud-free observations [1]. Two major efforts would be needed to further improve this accuracy. The first one concerns the improvement of PICS radiative properties characterisation. It is challenging as these PICS, such as Libya-4, are very remote locations making routine ground observation very challenging. Additionally, some radiative effects might have been neglected so far. For instance, some surface 3D effects might become non-negligible to reach accuracy lower than 3% [2]. The second one concerns the use of advanced radiative transfer models (RTMs). The use of RTMs for the simulation of satellite observations relies on a series of built-in feature such standard atmospheric profiles, rescaling of molecular concentration or the calculation of atmospheric layer mean optical properties. The use of different radiative transfer models using similar input to characterise surface and aerosol properties can lead to different results as shown in Figure 1 where Aqua-MODIS data acquired over the CEOS Pseudo Invariant Calibration Site (PICS) Libya-4 have been simulated with four different RTMs using the same surface and aerosol models. As can be seen, the magnitude of the mean relative bias between observations and simulations depends on the radiative transfer model. The range of bias differences among the models is about 2% to 3% [1]. Similar differences have already been reported in other studies [3].

The difficulty for verification that a radiative transfer model can accurately represent a satellite observation should not underestimated. It is extremely challenging as it is very difficult to characterise all the observed scene properties exactly at the satellite overpass time. Model intercomparison represents therefore a useful exercise to assess simulation accuracy. Many initiatives have already been undertaken so far to compare models but none of them specifically focused on the simulation of satellite data.

doi: 10.25923/7kkg-vz09

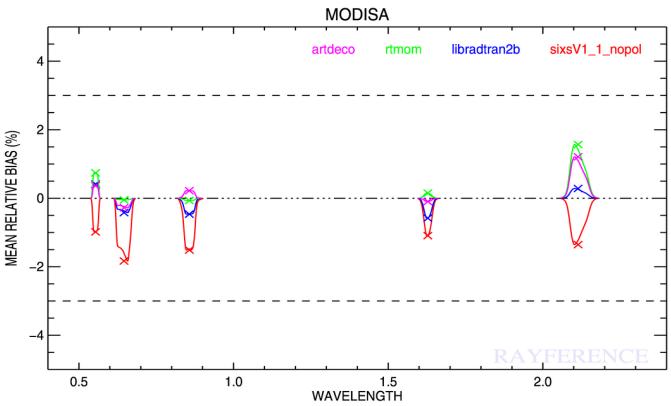

Figure 1: Mean relative differences (in %) between Aqua-MODIS observations acquired of Libya-4 CEOS PICS and simulations with four different radiative transfer models (ARTDECO, RTMOM, libradtran and 6SV).

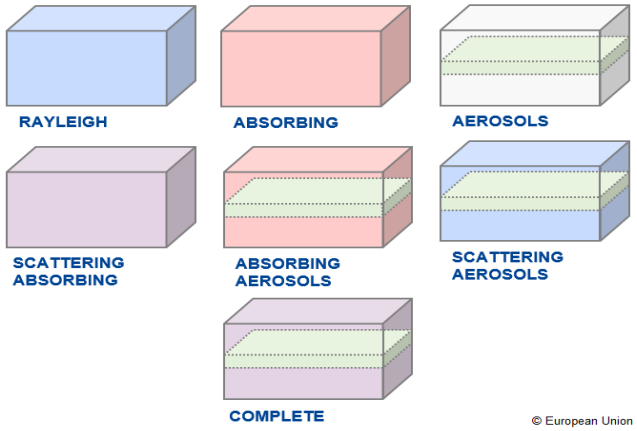

Figure 2: Atmosphere components combinations in RAM4ATM.

The RAMI4ATM initiative

RAMI4ATM is a new initiative dedicated to the benchmarking of coupled surface-atmosphere radiative transfer models. **RAMI4ATM** expands the RAdiation transfer Model Intercomparison (RAMI) initiative to the simulation of satellite observations organized by the Joint Research Centre of the European Commission [4]. Compared to current benchmarks, the major difference is that **RAMI4ATM** seeks to account for atmospheric radiative effects occurring between the surface and the simulated signal reaching a given spaceborne radiometer. Models participating in RAMI4ATM should support the simulation of radiative processes at the surface, in the atmosphere and account for the radiative coupling between the two (Figure 2).

Over the past decades, many radiative transfer models have been developed and are widely used in Earth Observation, e.g., vicarious calibration, lookup table generation for atmospheric correction or sensitivity analyses. Many of these models include atmospheric property databases. Subcomponents of these models have been extensively tested in ideal conditions but so far, no long-term initiative similar to RAMI has been undertaken to systematically compare models when they are used to simulate actual remote sensing observations. The uncertainties of these models have not been clearly assessed in **realistic usage conditions** when supporting typical Earth Observation applications by remote sensing scientists.

This new phase is oriented toward the support of calibration and validation activities relying on the use of radiative transfer models for the simulation of satellite observations in the visible, near and shortwave infrared spectral regions. It is therefore primarily directed at model users involved in calibration and validation activities. Participation from radiative transfer model developers is however also welcome. They are referenced as expert users in RAMI4ATM.

RAMI4ATM covers various scenarios resulting from a combination of surface and atmospheric properties. Specifically, the following cases are foreseen:

- A standard atmospheric profile is considered with the possibility to rescale the water vapor and ozone total column concentration.
- Small and large particles aerosol types with different low and high optical thickness;A total of eight surfaces are foreseen: three lambertian surfaces, two anisotropic surfaces and three homogeneous discrete canopies with isotropic background and different leaf angle distributions (LAD).

Expected outcome

As well as for RAMI-1, the primary goal of RAMI4ATM will be to document the variability between coupled surface-atmosphere models when run under well-controlled, but realistic, conditions. The expected outcome of this exercise is as follows: to allow users to cross compare their simulations with respect to the other participating models over a variety of ideal atmospheric scenarios including gas absorption, Rayleigh and Mie scattering;

(1) to inform the user community on the performance of the participating available models and the differences in their results;
(2) to help developers improve their models;
(3) to progressively build community consensus on the best ways to

simulate the radiative transfer below and above the Earth's atmosphere.

GSICS scientists involved in radiative transfer modelling in support of calibration verification activities are highly encouraged to participate in RAMI4AT (https://rami-benchmark.jrc.ec.europa.eu/)

References

[1] Govaerts, M. Y. *Estimating the accuracy of 1D radiative transfer models over the Libya-4 site*. 15 https://www.eradiate.eu/resources/docs/reports/report-assessment_calibration_libya4-2.3-20191007.pdf (2019).

[2] Govaerts, Y. M. Sand Dune Ridge Alignment Effects on Surface BRF over the Libya-4 CEOS Calibration Site. *Sensors* **15**, 3453–3470 (2015).

[3] Vicent, J. *et al.* Comparative analysis of atmospheric radiative transfer models using the Atmospheric Look-up table Generator (ALG) toolbox (version 2.0). *Geoscientific Model Development* **13**, 1945–1957 (2020).

[4] Pinty, B. *et al.* Radiation transfer model intercomparison (RAMI) exercise. *J. Geophys. Res.* **106**, 11,937-11,956 (2001).

Radiometric cross-calibration of the ZY1-02D hyperspectral imager using the GF-5 AHSI imager

By C. Niu, K. Tan, X. Wang (East China Normal University), B. Han (Institute of Remote Sensing Satellite, China Academy of Space Technology), S. Ge (China Centre for Resources Satellite Data and Application), P. Du (Nanjing University) and F. Wang (Fudan University)

Recently, an article was published in IEEE TGRS in 2021[1], which introduces a cross-calibration method to calibrate the ZY1-02D hyperspectral imager using the well-calibrated Gaofen-5 Advanced Hyperspectral Imager. The 6S radiative transfer model is selected to simulate the apparent reflectance of the two hyperspectral sensors, and the calibration coefficients are calculated by spectral channel matching. This method could be used as an effective supplement to the on-orbit calibration method, and could also be extended to other satellite hyperspectral imagers.

Introduction

With the development of high-resolution satellite technology, China has launched a series of remote sensing satellites carrying hyperspectral imagers. On 9 May 2018, China launched the Gaofen-5 (GF-5) satellite with the Advanced Hyperspectral Imager (AHSI) carried onboard. The AHSI imager features 330 spectral channels covering a solar reflective range of 400–2500 nm, with a spatial resolution of 30 m [2]. On 12 September 2019, China launched the first civil hyperspectral satellite—ZY1-02D satellite. The ZY1-02D hyperspectral imager features 166 spectral channels, and has a 60-km swath width. It has the same spectral range and spatial resolution as the AHSI imager.

Cross-calibration methods have been proposed to replace in situ measurement by using concurrently collected images from a well-calibrated sensor. In order to ensure the accuracy of cross-radiometric calibration, there is a higher requirement for the spectral resolution of the reference imagers. The GF-5 AHSI imager has a higher spectral resolution and can be used as the reference sensor for the cross-calibration of the ZY1-02D hyperspectral imager [3].

Here we focus on providing timely and accurate radiometric calibration coefficients after satellite launch. Accordingly, a radiative transfer modeling method was utilized to calibrate the ZY1-02D hyperspectral imager. Reflectance-based vicarious calibration was carried out to verify the radiometric accuracy.

Method

According to the principle of radiation transmission, the relationship between the TOA reflectance and the TOA radiance can be expressed as follows [4]:

$$\rho_{TOA}(\lambda) = \frac{\pi \cdot L(\lambda) \cdot d^2}{E_s(\lambda) \cdot \cos\theta_s} \quad \ldots\ldots(1)$$

where L is the TOA radiance, d is the earth–sun distance, θ_s is the solar zenith angle, and E_s is the solar radiation at the TOA.

doi: 10.25923/7kkg-vz09

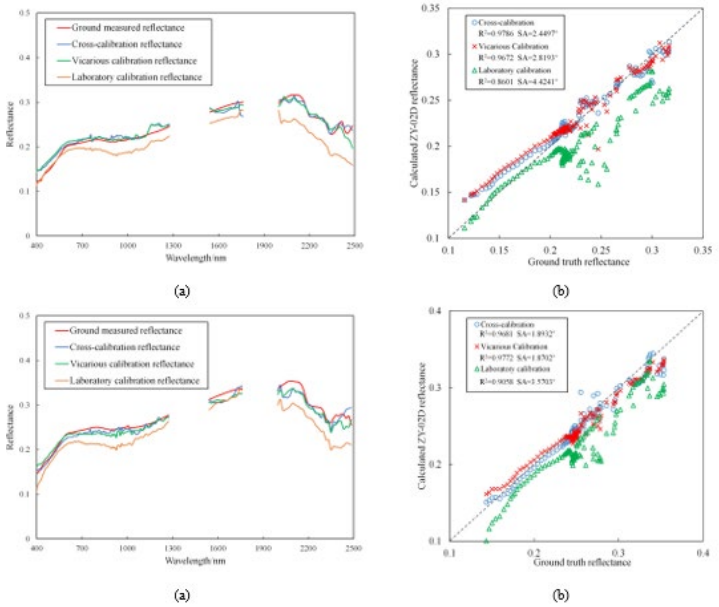

Figure 1: The calibration results and the ground-measured reflectance at the Dunhuang site on 19 August 2020. (a) Spectral curves of the surface reflectance result from 400 to 2500 nm on 30 May 2020. (b) Scatter plots and accuracies of the three calibration results on 30 May 2020. (c) Spectral curves of the surface reflectance result from 400 to 2500 nm on 19 August 2020. (d) Scatter plots and accuracies of the three calibration results on 19 August 2020.

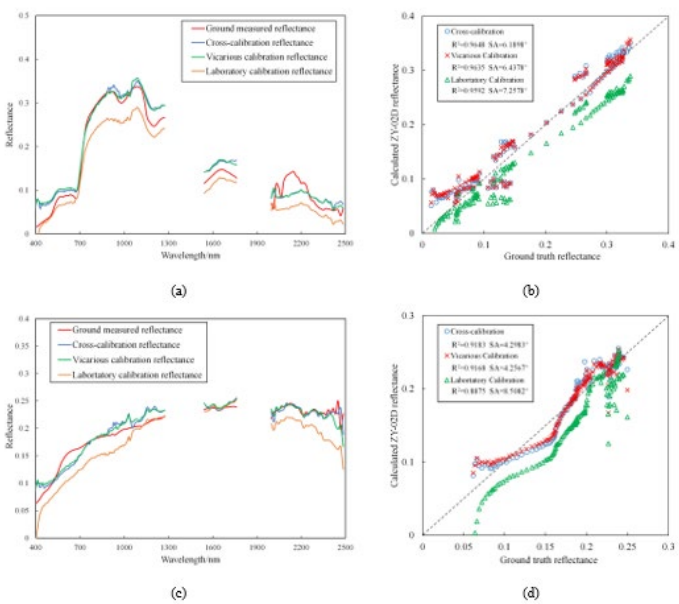

Figure 2: The calibration results for the paddy field and bare soil category and the ground-measured reflectance at the Xuzhou site on 19 October 2020. (a) Spectral curves of the paddy field. (b) Scatter plots and accuracies of paddy field. (c) Spectral curves of bare soil category. (d) Scatter plots and accuracies of bare soil.

For hyperspectral imagers, the values obtained in each channel are related to the spectral response function. The 6S radiative transfer model was selected to simulate the apparent reflectance of the two hyperspectral sensors under corresponding imaging conditions. The relationship between the reference sensor and the sensor to be calibrated can be obtained as follows:

$$\frac{L_C}{L_R}=\frac{\int_C S(\lambda)f_C(\lambda)d\lambda\cdot\int_R S(\lambda)d\lambda\cdot\rho_{TOA\_C}\cdot\cos\theta_{S\_C}}{\int_R S(\lambda)f_R(\lambda)d\lambda\cdot\int_C S(\lambda)d\lambda\cdot\rho_{TOA\_R}\cdot\cos\theta_{S\_R}}. \quad \ldots\ldots(3)$$

The Gaussian response function spectral response functions were used for spectral channel matching, and the TOA radiance of the sensor to be calibrated can be expressed as follows:

$$L_{i,C}=L_{i,R}\frac{\rho_{i,TOA\_C}\cdot\cos\theta_{S\_C}}{\rho_{i,TOA\_R}\cdot\cos\theta_{S\_R}} \quad \ldots.(4)$$

where $L_{i,c}$ and ρ_{i,TOA_C} are, respectively, the TOA radiance and TOA reflectance of the sensor to be calibrated in channel *i*. $L_{i,R}$ and ρ_{i,TOA_R} are, respectively, the TOA radiance and TOA reflectance of the reference sensor after interpolation in channel *i*.

The relationship between the DN value and the TOA radiance can be expressed as follows:

$$L_i=a_iDN_i+b_i \quad \ldots..(5)$$

where a_i is the gain coefficient in band *i*, b_i is the offset value in band *i*.

Results

After radiometric calibration using the cross-calibration coefficients and vicarious calibration coefficients, the surface reflectance was obtained through atmospheric correction. The laboratory radiometric calibration coefficients were also used for judging and evaluating the sensor radiation attenuation. Fig. 1 shows the comparison results obtained at the Dunhuang site. It can be seen that the calibration reflectance spectra for the ZY1-02D imager show a high degree of consistency. The accuracy of the laboratory calibration results is the poorest. The cross-calibration reflectance spectra are also highly consistent with the ground-measured reflectance, and the accuracy is similar to that of the vicarious calibration results. To verify the performance of the calibration coefficients for different types of ground features, we carried out verification of the results in two different land-cover types: paddy field and bare soil.

From the trend of the spectral curve and the extreme value of reflectance shown in Fig. 2, the reflectance results of ZY1-02D are basically consistent with the measured reflectance.

doi: 10.25923/7kkg-vz09

The deviation between the laboratory calibration reflectance and the measured reflectance is again the largest. The results of the cross-validation for these two ground features are slightly better than those of the vicarious calibration, which shows the reliability of the proposed cross-calibration method. The comparison of the results is shown in Table I.

Validation site	Ground feature	Calibration method	R^2	Spectral angle°
Dunhuang 30 May 2020	Calibration site	Cross-calibration	0.9786	2.4497
		Vicarious calibration	0.9672	2.8193
		Laboratory calibration	0.8601	4.4241
Dunhuang 19 August 2020	Calibration site	Cross-calibration	0.9681	1.8932
		Vicarious calibration	0.9772	1.8702
		Laboratory calibration	0.9058	3.5703
Xuzhou 19 October 2020	Paddy field	Vicarious calibration	0.9648	6.1898
		Laboratory calibration	0.9635	6.4378
		Laboratory calibration	0.9592	7.2578
Xuzhou 19 October 2020	Bare soil	Vicarious calibration	0.9183	4.2983
		Laboratory calibration	0.9168	4.2567
		Laboratory calibration	0.8875	8.5082

Table 1: Comparison of the results of the different calibration methods

Conclusion

In this study, the GF-5 AHSI imager with a high spectral resolution after precise radiometric calibration was utilized for the cross-calibration of the ZY1-02D hyperspectral imager, and the calibration results were compared with those of the laboratory calibration method and vicarious calibration method. The reliability of the cross-calibration method was verified using multiple measured surface reflectance data sets. It was found that the results of the laboratory calibration are no longer suitable for the space environment, and the calculated reflectance was found to be quite different from the measured surface reflectance. The ZY1-02D hyperspectral imager calibrated by both the cross-calibration method and the vicarious calibration method showed a stable radiometric performance.

The results of the cross-calibration and vicarious calibration were similar. In the four groups of validation experiments, three groups of experiments reported cross-calibration results that were better than the vicarious calibration results, which shows the reliability of the cross-calibration method. In the future, we will consider predicting the overlapping imaging area in advance, and collect the meteorological data and the spectral data in situ for accurate calibration and verification.

References:

[1] C. Niu, K. Tan, X. Wang, B. Han, S. Ge, P. Du, and F. Wang, "Radiometric Cross-Calibration of the ZY1-02D Hyperspectral Imager Using the GF-5 AHSI Imager," *IEEE Transactions on Geoscience and Remote Sensing,* vol. 60, pp. 1-12, 2021.

[2] Y. N. Liu, D. X. Sun, X. N. Hu, X. Ye, Y. D. Li, S. F. Liu, K. Q. Cao, M. Y. Chai, W. Y. N. Zhou, J. Zhang, Y. Zhang, W. W. Sun, and L. L. Jiao, "The Advanced Hyperspectral Imager Aboard China's GaoFen-5 satellite," *Ieee Geoscience and Remote Sensing Magazine,* vol. 7, no. 4, pp. 23-32, Dec, 2019.

[3] K. Tan, X. Wang, C. Niu, F. Wang, P. Du, D.-X. Sun, J. Yuan, and J. Zhang, "Vicarious calibration for the AHSI instrument of Gaofen-5 with reference to the CRCS Dunhuang test site," *IEEE Transactions on Geoscience and Remote Sensing,* vol. 59, no. 4, pp. 3409-3419, 2020.

[4] B.-C. Gao, K. B. Heidebrecht, and A. F. Goetz, "Derivation of scaled surface reflectances from AVIRIS data," *Remote sensing of Environment,* vol. 44, no. 2-3, pp. 165-178, 1993.

doi: 10.25923/7kkg-vz09

NEWS IN THIS QUARTER

22nd GSICS Executive Panel Meeting (GSICS-EP-22) held virtually from 10-11 May, 2022

By Mitch Goldberg (NOAA), Kenneth Holmlund (WMO), Heikki Pohjhola (WMO), Lawrence Flynn (NOAA), Manik Bali (UMD), Kamaljit Ray (IMD) and Fangfangu Yu (UMD)

The 22nd Session of the Global Space-based Inter-Calibration System Executive Panel (GSICS-EP-22) was held as an online meeting on 10-11 May 2022, prior to the Working Group meetings of the Coordination Group for Meteorological Satellites (CGMS) at CGMS-49. The meeting was hosted via web by WMO and supported by the GSICS Coordination Center at NOAA. Over 25 GSICS members participated in the meeting representing CMA, ESA, EUMETSAT, IMD, ISRO, JAXA, JMA, KMA, MOES, NASA, NIST, NOAA, SITP, USGS, GCC, GDWG, GRWG and WMO. This included EP members from 13 GSICS member agencies, members of WMO secretariat, GSICS Coordination Center, and Chairs of GSICS Groups and Subgroups.

The meeting began with a review of the proposed agenda by WMO and approval by the meeting attendees. The EP welcomed Dr. Xiaoxiong Xiong representing NASA and Dr. Bojan Bojkov representing EUMETSAT as new members of the EP.

Following these actions, the GSICS Coordination Center (GCC) Director, Larry Flynn, reported activities for the previous year and goals for the coming year. He thanked members for participation in the GSICS Annual Meeting in March 2022. He mentioned that the interest in GSICS continues to be strong with almost 420 persons registered for the messaging service. He highlighted that over 70 scientists contributed to articles in the GSICS Newsletter as the newsletter continues to be received very well by the community and beyond. Last year, GCC published a special issue on the State of Observing System. GCC also initiated discussions on how to make products better and more accessible. Larry also briefed on new actions that GCC picked up earlier this year in the annual meeting 2022.

GSICS Research Working Group (GRWG) Chair, Fangfang Yu, presented a summary of GRWG activities over the past year. She reported that 2022 GRWG annual (virtual) meeting was successfully held on 10 March and 14-18 March in 2022, with strong support from EP, GCC, GDWG, and GRWG members. More than 65 people from international space and operational agencies, research institutes, universities, and private sectors attended the meetings. The mini-conference session in the annual meeting resumed this year, after a two-year gap due to the global pandemic. Over the past year, GRWG subgroups have continued active research and technical discussions and collaborations via regular web meetings. The GRWG also coordinated with the member agencies to prepare the 2022 GSICS state of observing system which was reported on 11 May 2022.

GRWG Subgroups reported on the status of their activities. The GRWG infrared (IR) Subgroup reported that the subgroup has been highly active in several areas including expansion of the group from GEO/LEO inter-calibration to GEO/GEO, LEO/LEO comparisons and generating datasets. They are also working with hyperspectral sounder inter-calibration, reprocessing of measurement, gap filling and collocation topics. A new IR subgroup chair is needed when the three years' term is completed. The subgroup has plans to set up bi-monthly or monthly web meetings, and support more cross-community efforts with other entities, e.g., ISSCP-NG, the NWP community and the CEOS WGVS. In the future codes will be hosted in GitHub and GSICS wiki.

The VIS/NIR subgroup recommended migrating from Aqua-MODIS to N20-VIIRS as a VIS reference instrument and from Thuillier 2003 to TSIS-1 HSRS (Link) for solar spectra. They are working with CEOS IVOS to coordinate the recommendations. They are also coordinating with CLARREO Path Finder (PF) group to organize a CLARREO and GSICS meeting dedicated to intercalibration for NOAA-20 VIIRS and CERES after CLARREO PF's first year of operations. The VIS/NIR subgroup's goals are to accomplish DCC visible channel GSICS correction product, best practices, DCC SWIR channel calibration product and GSICS visible calibration product. The 4th Lunar calibration workshop is planned to take place in November 2023 after lunar model inter-comparison exercise and report then results. The Microwave (MW) subgroup reported as general achievement improvements in MW calibration and geolocation approaches and in instrument performance monitoring and uncertainty

characterization improvements. They have also facilitated the GSICS spectral response function format discussion and are collecting feedback. As main outcomes they reported that frequency parameter should be added to improve backward compatibility of the format and to use arrays minimizing the number of variables. As planned activities in 2022 they reported possible collaboration activities related to MW lunar calibration and geolocation assessment, inter-calibration of SmallSat / Cubesat data from TROPICS, TEMPEST-D with operational sounders, NWP sensitivity analysis from MWTS-III FY-3E early morning orbit data and to obtain TROPICS CubeSat lunar data obtained from its "sky-scan". They expect to deliver, in 2022, the data base associated with the lunar disk-average brightness temperature for the MW frequency range between 23 and 183 GHz, inter-calibration statistics between operational MW sounders and SmallSat / CubeSat L1b products and related to GSICS products MW FCDR time series.

The UVN subgroup (UVNS) featured talks on the status of calibration and validation for most of the operational and planned UV/VIS spectrometers including radiance and irradiance measurements from FY-3F/OMS, NIER GEMS, TROPOMI, Metop (GOME-2, S4/UVN and S5/UVNS), JPSS (S-NPP & NOAA-20 OMPS), DSCOVR / EPIC, TEMPO, and EOS Aura OMI. The OMPS, OMI and GOME-2 teams are reprocessing long-term records with improved consistency in the calibration characterization. The GEMS instrument is operating in a GEO orbit and provides new opportunities for GEO/LEO comparisons for LEO UV and Visible spectrometers. Significant calibration comparisons are taking place among the LEO instruments, and the GEMS instrument's measurements are providing the first opportunities to use LEO/GEO comparisons for this class of sensors.

The GSICS Data Working Group (GDWG) reported several key activities by GSICS member agencies. These included ESA's EVDC website and salinity website that aim to help the calibration community with state-of-the-art calibration data. The Data Working Group also informed the EP about the reprocessing activity by CMA wherein they deployed GSICS corrections on a massive data base dating back decades and reprocessed the entire Earth Observation data obtained from Chinese Satellites. Detailed presentations on these topics were given at the recently concluded GSICS Annual meeting and detailed discussions and actions generated are documented in the minutes of the Annual Meeting. GDWG also listed a series of tools that are available on the cloud and Github for the community to use. The EP-22 also nominated Manik Bali to serve as Vice Chair of the Data Working Group.

Over the years the GSICS EP has placed special stress on developing relationships with potential user communities. This year Andy Heidinger (NOAA), who is leading the International Satellite Cloud Climatology Project (ISCCP), was invited to present potential requirements and expectations from GSICS community from-which ISCCP can benefit. Andy indicated that ISCCP has pioneered in the development of multi-decadal cloud climate records (1983-present) from the operational meteorological geostationary imagers. https://www.ncdc.noaa.gov/isccp. In a few years, the entire globe will be encircled by a new generation of advanced geostationary imagers (ABI, AHI, AMI, FCI, AGRI, GXI, etc.). However, it would add tremendous value if GSICS corrected observations of the GEO imagers are used instead of native measurements.

Andy mentioned that the Next Generation of the International Satellite Cloud Climatology Project (ISCCP-NG) is proposed by GEWEX as a follow-on to the classic ISCCP to capitalize on these new capabilities. ISCCP-NG has developed Level–1 Gridded Data (L1G) which is a composite of (L1B) images taken by global geostationary satellites. L1G data is available via ftp for GOES-16/17, Meteosat 11/8, Himawari-8 since 2020. The ISCCP-NG website was launched: https://cimss.ssec.wisc.edu/isccp-ng/ and L2 testing of L1G has started with Martin Stengel (DWD). ISCCP is set to use the GSICS calibrated BT's in each of the L1B images taken by the geostationary satellites can generate the L1G composite. They have started looking at the GSICS product Users Guide provided by EUMETSAT. It was decided that ISCCP would be included as a part of a new subgroup in GSICS. This would help to connect GSICS directly with users of its products, deliverables and algorithms.

D.GEP.20220510.3: GSICS to include application sub-group in their structure including ISCCP

Heikki Pohjola spoke about the recent activities at WMO which includes the Unified Policy for International Exchange of Earth System Data. He explained the major changes compared to old WMO Data Policy resolutions 40, 25 and 60. The important change is that with the new data policy WMO commits itself to broadening and enhancing the free and unrestricted international exchange of Earth system data. Heikki also mentioned about the key role WIGOS framework is playing in streamlining data pipelines in WMO and integrating various observing platforms. He provided the status of the

doi: 10.25923/7kkg-vz09

WMO GSICS website. He also introduced the WMO plan to organize an industry day event during Q4/2022 inviting all the companies working in space-based Earth observations and CubeSats/mini satellites.

E. Talaat(NOAA), provided a summary of the Space Weather activities to the EP. Responding to A.GEP.20200519.13, Talaat, mentioned that further discussion is needed for data sharing. The inclusion of space weather as a subgroup within GRWG was discussed. It was agreed that space weather will be added under GRWG as provisional for the next two years.

D.GEP.20220510.7: GSICS to set up provisional sub-group for Space Weather under GRWG with the list of members.The EP-22 meeting concluded with GCC Director Larry Flynn volunteering to arrange for NOAA to host the GSICS Annual Meeting in 2023 at NOAA's NCWCP in College Park MD with the capability for hybrid attendance.

GSICS-EP-22 meeting presentation and related documents are available at **https://community.wmo.int/meetings/gsics-ep-22** .

Announcements

AOMSUC-12 to be held online 11-18 November 2022

By Allen Huang, SSEC, University of Wisconsin-Madison

The 12th Asia-Oceania Meteorological Satellite Users' Conference (AOMSUC-12) will be held virtually on 11-18 November 2022. Details can be found on the conference web page, including the first announcement and the registration information: https://www.data.jma.go.jp/mscweb/en/aomsuc12/index.html .

The theme of AOMSUC-12 will be "Full Exploitation of Today's Advanced Global Meteorological Satellite Observing System".

The AOMSUC-12 will consist of two days training workshop that focuses on the application of current satellite data for meteorological and climatological applications, three days of AOMSUC plenary session, and a Joint Meeting of RA II WIGOS Project and RA V TT-SU for RA II and RA V NMHSs.

11th and 14th November 2022:

Training event on satellite data and product application

15th – 17th November 2022:

The 12th Asia-Oceania Meteorological Satellite Users' Conference

18th November 2022:

Joint Meeting of RA II WIGOS Project and RA V TT-SU for RA II and RA V NMHSs (by invitation).

The deadline for submission is 30th September 2022. There is no fee required for the AOMSUC-12 attendee or presenter. Please forward this announcement to all your colleagues to keep the dates aside for participation and continue your great tradition to contribute to our community.

GSICS-Related Publications

Angal, Amit, Carol Bruegge, Xiaoxiong Xiong, and Aisheng Wu. 2022. 'Intercalibration of the Reflective Solar Bands of MODIS and MISR Instruments on the Terra Platform'. *Journal of Applied Remote Sensing* 16 (2): 1–13. https://doi.org/10.1117/1.JRS.16.027501.

Flynn, Lawrence E., ed. 2022. 'Role of GSICS in NWP Satellite Data Assimilation'. *JCSDA Quarterly*, no. 71. https://doi.org/10.25923/chqf-pb23.

Niro, F.; Goryl, P.; Dransfeld, S.; Boccia, V.; Gascon, F.; Adams, J.; Themann, B.; Scifoni, S.; Doxani, G. European Space Agency (ESA) Calibration/Validation Strategy for Optical Land-Imaging Satellites and Pathway towards Interoperability. *Remote Sens.* **2021**, *13*, 3003. https://doi.org/10.3390/rs13153003

Protat, A., Louf, V., Soderholm, J., Brook, J., and Ponsonby, W.: Three-way calibration checks using ground-based, ship-based, and spaceborne radars, Atmos. Meas. Tech., 15, 915–92610.5194/amt-15-915-2022.

Wang, T., J. Zeng, K. Chen, Z. Li, H. Ma, Q. Chen, H. Bi, P. Shi, L. Zhu, and C. Cui. 2022. 'Comparison of Different Intercalibration Methods of Brightness Temperatures from FY-3D and AMSR2'. *IEEE Transactions on Geoscience and Remote Sensing*, 1–1. https://doi.org/10.1109/TGRS.2022.3176748.

Zhang, Wen-Liang, and Geng-Ming Jiang. 2022. 'Intercalibration of FY-3C MWRI Over Forest Warm-Scenes Based on Microwave Radiative Transfer Model'. *IEEE Transactions on Geoscience and Remote Sensing* 60: 1–11. https://doi.org/10.1109/TGRS.2021.3086801.

Submitting Articles to the GSICS Quarterly Newsletter

The GSICS Quarterly Press Crew is looking for short articles (800 to 900 words with one or two key, simple illustrations), especially related to calibration / validation capabilities and how they have been used to positively impact weather and climate products. Unsolicited articles may be submitted for consideration anytime, and if accepted, will be published in the next available newsletter issue after approval / editing. Please send articles to manik.bali@noaa.gov.

With Help from our friends:

The GSICS Quarterly Editor would like to thank Dave Doelling (NASA), Tim Hewison (EUMETST) and Lawrence Flynn (NOAA) for reviewing articles in this issue. Thanks are due to Jan Thomas (NOAA) for helping with 508 compliance.

Published By

GSICS Coordination Center
NOAA/NESDIS/STAR NOAA
Center for Weather and Climate Prediction,
5830 University Research Court
College Park, MD 20740, USA

CISESS
5825 University Research Court, Suite 4001,
University of Maryland, College Park, MD 20740-3823